Numerical methods for weak solution of wave equation with van der Pol type boundary conditions ☆

Jun Liu[a], Yu Huang[b], Haiwei Sun[c], Mingqing Xiao[a,*]

[a] *Department of Mathematics, Southern Illinois University, Carbondale, IL 62901, USA*
[b] *Department of Mathematics, Zhongshan (Sun Yat-Sen) University, Guangzhou, China.*
[c] *Department of Mathematics, University of Macau, Macao, China.*

Abstract

We develop numerical methods for solving wave equation with van der Pol type nonlinear boundary conditions under the framework of weak solution. Based on the wave reflection on the boundaries, we first solve the Riemann invariants by constructing two iteration mappings, and then show that the weak solution can be obtained by the integration of the Riemann invariants on the boundaries. If the compatible conditions are not satisfied or only hold with a low degree, a high order integration method is developed for the numerical solution. When the initial condition is sufficiently smooth and compatible conditions hold with a sufficient degree, we establish a sixth-order finite difference scheme, which only needs to solve a linear system at any given time instance. Numerical experiments are provided to demonstrate the effectiveness of the proposed approaches.

Keywords: Wave equation; van der Pol type boundary condition; weak solutions; chaotic behavior; numerical integration; finite difference.

1. Introduction

We consider the numerical solution of the one-dimensional wave equation system associated with van der Pol boundary condition in the form of

$$\begin{cases} w_{tt} - w_{xx} = 0, \quad x \in (0,1),\ t > 0, \\ w_x(0,t) = -\eta w_t(0,t), \quad \eta \neq 1, \qquad t > 0, \\ w_x(1,t) = \alpha w_t(1,t) - \beta w_t^3(1,t), \quad 0 < \alpha < 1,\ t > 0, \\ w(x,0) = w_0(x), \qquad w_t(x,0) = w_1(x), \qquad 0 < x < 1, \end{cases} \tag{1.1}$$

where α, β, and η are given real constants. When $\eta = 1$, the system (1.1) is not well-posed. Thus throughout this paper we assume $\eta \neq 1$. The wave equation

☆Project was supported in part by National Natural Science Foundation of China (Grants No. 11071263) and in part by NSF 1021203 of the United States. Paper is submitted to *Journal of Computational Physics.*

*Corresponding author.

Email addresses: junliu2010@siu.edu (Jun Liu), stshyu@mail.sysu.edu.cn (Yu Huang), hsun@umac.mo (Haiwei Sun), mxiao@siu.edu (Mingqing Xiao)

itself is linear and represents the infinite-dimensional harmonic oscillator. The right-handed side boundary condition (at $x = 1$) is nonlinear when $\beta \neq 0$, which is usually called a *van der Pol* type boundary condition (see, e.g., [? ? ? ? ? ? ? ? ? ? ? ? ? ? ?]). The left-handed side boundary condition (at $x = 0$) is linear, where $\eta > 0$ indicates that energy is being injected into the system at $x = 0$. If we denote the total energy as

$$E(t) = \frac{1}{2}\int_0^1 |\nabla w(x,t)|^2 dx = \frac{1}{2}\int_0^1 \left[w_x^2(x,t) + w_t^2(x,t)\right] dx,$$

then by applying the boundary conditions we have

$$\frac{d}{dt}E(t) = \eta w_t^2(0,t) + w_t^2(1,t)[\alpha - \beta w_t^2(1,t)].$$

Thus if $\eta > 0$, the system (1.1) has a self-excited mechanism that supplies energy to the system itself. Moreover, any constant could be an equilibrium.

The PDE system (1.1) has received considerable attention since it exhibits many interesting and complicated dynamical phenomena, such as limit cycles and chaotic behavior of (w_t, w_x) when the parameters α, β and η assume certain values [? ? ? ?]. Different from dynamics of a system of ODEs, this is a simple and useful infinite-dimensional model for the study of spatio-temporal behaviors as time evolutes. For instance, the propagation of acoustic waves in a pipe satisfies the linear wave equation:

$$w_{tt} - w_{xx} = 0.$$

Its general solution is the d'Alembert solution

$$w(x,t) = F(x-t) + G(x+t),$$

where F, G are arbitrary functions. This solution describes a superposition of two traveling wave with arbitrary profiles, one propagating with unit speed to the left, the other with unit speed to the right. The boundary conditions appeared in (1.1) can create irregularly acoustical vibrations. This type of vibrations, for example, can be generated by noise signals radiated from underwater vehicles, and there are intensive research for the properties of acoustical vibrations in current literature (see e.g., [? ? ?]). Hence numerical study of this type of chaotic characteristics is not only important but also may lead to a better understanding of the dynamics of acoustic systems.

One challenge for solving (1.1) numerically results from the fact that the wave solution of (1.1), corresponding to certain real world phenomena, is not necessary to be smooth. For a given smooth initial condition (w_0, w_1) of (1.1), the necessary and sufficient condition for (1.1) to admit a classical solution $w \in C^2([0,1] \times [0,T])$ is that the initial condition (w_0, w_1) have to satisfy the so-called compatibility conditions

$$w_0'(0) = -\eta w_1(0), \qquad w_0'(1) = \alpha w_1(1) - \beta w_1^3(1) \tag{1.2}$$

$$w_0''(0) = -\eta w_1'(0), \qquad w_0''(1) = \alpha w_1'(1) - 3\beta w_1^2(1) w_1''(1). \tag{1.3}$$

If the compatibility requirement is not met, then no matter how smooth the initial conditions w_0 and w_1 will be, there is always a jump discontinuity in w along the characteristics of the system. Thus many existing high-order finite difference approaches may fail to work properly since the existence of higher derivatives is no loner to be guaranteed.

Even if the necessary compatibility requirement is satisfied, the finite difference approach for (1.1) still remains challenging. When parameters η and α take certain values, the gradient of w will present chaotic dynamics, which implies that in such cases the solution of (1.1) will be very sensitive to numerical errors. To illustrate it, we give the detailed description below.

Denote the total variation of a function f on a closed interval $I = [a, b]$ by

$$V_I(f) = \sup_{\triangle} \left\{ \sum_{i=0}^{n-1} |f(x_{i+1}) - f(x_i)| \right\},$$

where the sup is taken over all the partition

$$\triangle : \{x_0 = a < x_1 < x_2 < \cdots < x_n = b\}.$$

Let us consider the Riemann invariants of (1.1)

$$u(x,t) = \tfrac{w_x(x;t)+w_t(x;t)}{2}, \quad v(x;t) = \tfrac{w_x(x;t)-w_t(x;t)}{2}. \tag{1.4}$$

Then we have the following known result that has been shown by the second author of this paper.

Lemma 1.1. *[?] Let $\alpha \in (0,1)$ be a constant and $\eta_1 < \eta_0 < 1$ be defined as*

$$\eta_0 = \frac{3\sqrt{3} - (1+\alpha)}{3\sqrt{3} + (1+\alpha)}, \qquad \eta_1 = \frac{1}{\sqrt{\alpha^2+3} + \alpha}.$$

For every given $\beta > 0$, $0 < \alpha < 1$, there exists a class of initial data (u_0, v_0), satisfying the compatibility conditions

$$\begin{aligned} u_0'(0) + v_0'(0) &= -\eta[u_0(0) - v_0(0)], \\ u_0'(1) + v_0'(1) &= \alpha[u_0(1) - v_0(1)] - \beta[u_0(1) - v_0(1)]^3, \end{aligned}$$

with finite total variations $V_{[0,1]}(u_0)$ and $V_{[0,1]}(v_0)$, such that

(i) If either $0 < \eta < \eta_1$ or $\eta_1^{-1} < \eta < \infty$, then

$$\lim_{t\to\infty} [V_{[0,1]}(u(\cdot,t)) + V_{[0,1]}(v(\cdot,t))] < \infty;$$

(ii) If either $\eta_1 < \eta < \eta_0$ or $\eta_0^{-1} < \eta < \eta_1^{-1}$, then

$$\lim_{t\to\infty} V_{[0,1]}(u(\cdot,t)) = \infty, \qquad \lim_{t\to\infty} V_{[0,1]}(v(\cdot,t)) = \infty;$$

(iii) There exists a $\eta_c \in (\eta_1, \eta_0)$ *such that for any* $\eta \in [\eta_c, \eta_c^{-1}]$ *but* $\eta \neq 1$, *we have*

$$V_{[0,1]}(u(\cdot,t)) = O(\exp(c_1 t)), \qquad V_{[0,1]}(v(\cdot,t)) = O(\exp(c_2 t)),$$

for some positive constants c_1 *and* c_2. *That is, the growth rates of the total variation of* $u(\cdot,t)$ *and* $v(\cdot,t)$ *are exponential as* $t \to \infty$.

In Lemma 1.1, conclusions (ii) and (iii) imply that (u, v) may behavior very irregularly even when the initial data (u_0, v_0) are very regular. The total variation of $u(\cdot,t)$ and $v(\cdot,t)$ being large indicates that u and v undergo rapid fluctuations. Moreover, conclusion (iii) states that the growth rates of the total variation of $u(\cdot,t)$ and $v(\cdot,t)$ may be exponential under certain circumstances, which corresponds to chaotic dynamics of (u, v) [**?**]. Since (w_x, w_t) is topologically conjugate to (u, v), (u, v) is equivalent to (w_x, w_t). Hence, chaotic w_x and w_t will be very sensitive to computation errors, and thus those traditional high-order finite difference approximations to w_x and w_t will not be able to provide a satisfactory accuracy. Figure 1 depicts such a chaotic scenario of w_x and w_t.

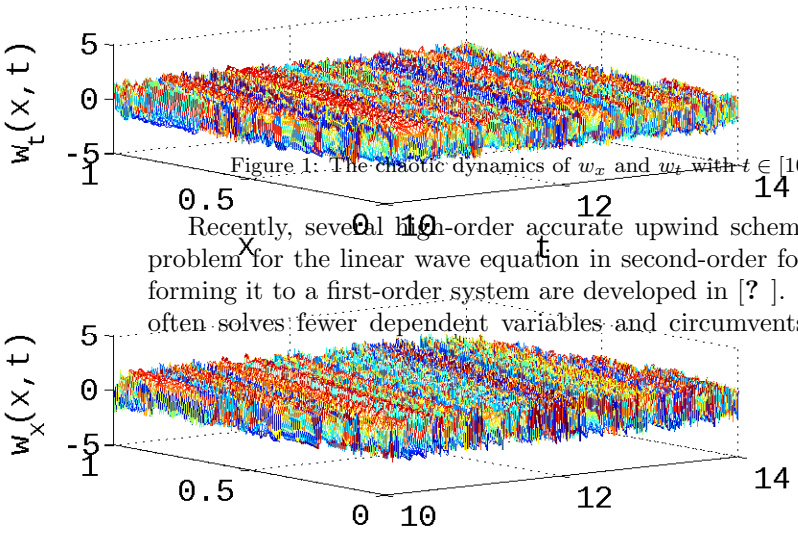

Figure 1: The chaotic dynamics of w_x and w_t with $t \in [10, 14]$ (Example 4).

Recently, several high-order accurate upwind schemes for the initial value problem for the linear wave equation in second-order form without first transforming it to a first-order system are developed in [**?**]. Such a direct approach often solves fewer dependent variables and circumvents the possible troubles

related to the equivalence, or lack thereof, between the first- and second-order systems. In general, first-order systems derived from second-order equations can admit a wider class of solutions, but such an approach may lead to some additional constraints in some cases. In [**?** **?**] the authors proposed high order finite difference approximations for the linear wave equation with discontinuous coefficients, where the global domain is first splitted at those discontinuities into sub-domains, and then perform discretization on each sub-domain using summation by parts operators before patch them together back using a projection method [**?**] or a penalty method[**?**]. However, existing numerical methods in current literature, including those mentioned above, are not suitable for solving system (1.1) discussed in this paper due to the nonlinear boundary condition of the system. Moreover, the inherent feature of (1.1)—the generated waves not necessary being smooth or even continuous, requires us to consider its solutions under the framework of weak (generalized) solutions. Our proposed approach, boundary integration method, renders us to obtain the weak solution with high accuracy and low compuational cost. Furthermore, if the wave solution is smooth enough, a high-order implicit finite difference scheme is developed with a fast convergence. The "implicit" idea here is to combine the unknowns and their derivatives over neighboring grid points to derive high-order approximations (see, for example, [**?**]). Such implicit schemes include combined compact difference schemes, which have been successfully applied to both steady and unsteady convection–diffusion equations [**?** **?** **?**]. Our proposed scheme is similar to the one developed in [**?**] for solving heat equations in the time direction, while in this paper we adopt it for solving (1.1) in terms of the spatial variable based on our theoretical development. To the best of our knowledge, effective numerical method for solving system (1.1) has not been seen in current literature.

As a starting point, we consider a simple, classical second-order central finite difference scheme for (1.1) provided that the system has a classical solution. Let $T > 0$ denote the terminal time for simulation. We first discretize the physical domain $[0, 1] \times [0, T]$ with $(N + 1) \times (M + 1)$ uniform grid points

$$x_n = n\Delta x, \quad \Delta x = \frac{1}{N}, \quad n = 0, 1, 2, \cdots, N,$$
$$t_k = k\Delta t, \quad \Delta t = \frac{T}{M}, \quad k = 0, 1, 2, \cdots, M,$$

and then solve the approximate solution $w_n^k \approx w(x_n, t_k)$ over all grid points (x_n, t_k). By the centered finite difference approximations for second derivatives, we obtain a discretized explicit scheme to the wave equation

$$\frac{w_n^{k+1} - 2w_n^k + w_n^{k-1}}{\Delta t^2} = \frac{w_{n+1}^k - 2w_n^k + w_{n-1}^k}{\Delta x^2}$$

with truncation error $O(\Delta t^2) + O(\Delta x^2)$. Similarly, discretization of the bound-

ary conditions gives

$$\begin{array}{rcl} \frac{w_1^k - w_{-1}^k}{2\Delta x} & = & -\eta \frac{w_0^{k+1} - w_0^{k-1}}{2\Delta t} \\ \frac{w_{N+1}^k - w_{N-1}^k}{2\Delta x} & = & \alpha \frac{w_N^{k+1} - w_N^{k-1}}{2\Delta t} - \beta \left(\frac{w_N^{k+1} - w_N^{k-1}}{2\Delta t} \right)^3 . \end{array} \tag{1.5}$$

The first initial condition provides $w_n^0 = w_0(x_n)$. The second initial condition is approximated by

$$\frac{w(x, 0 + \Delta t) - w(x, 0 - \Delta t)}{2\Delta t} = w_1(x)$$

for which

$$w_n^{-1} = w_n^1 - 2\Delta t w_1(x_n).$$

Now, it is not difficult to see from (1.5) that one has to solve a cubic polynomial to get w_N^{k+1} for each $k \geq 1$, which results in solving a nonlinear finite difference equation. If (1.1) does not admit a classical solution, then this approach cannot give the desirable solution with second order accuracy.

The main contributions of this paper are given below:

1. Inspired by [**? ?**], we establish two interval mappings that incorporate the boundary conditions and can characterize the dynamics of the Riemann invariants (1.4) and the explicit iterative representation for $(u(x,t), v(x,t))$ is obtained for $t \geq 0$.

2. Then we show that for a given initial condition $(w_0, w_1) \in L^\infty([0,1]) \times L^\infty([0,1])$, the weak solution $w \in L^\infty([0,1] \times [0,\infty))$ can be expressed as

$$w(x,t) = \int_x^{t+x} u(0,\tau) d\tau - \int_{1-x}^{1-x+t} v(1,\tau) d\tau + w_0(x).$$

   Here the initial condition (w_0, w_1) may not satisfy the compatible condition. This expression allows us to use advanced integration methods such as adaptive quadrature method to obtain the numerical solution with high accuracy. Different from classical finite difference method, the proposed approach does not require to solve the equation on spatial grid points, instead, it only needs to compute the integrations on the boundary. Thus our approach not only significantly reduces the regularity requirement for the solution but also has low computational complexity.

3. Moreover, our proposed approach allows us to obtain the numerical solution near the final time T that depends on little prior inner grid solution. Hence the proposed approach is quite efficient when the computation of long-term dynamics is required.

4. Furthermore, if compatibility conditions hold with a sufficient degree, then based on the representation of u and v that include the underlying boundary conditions, we develop a sixth-order finite-difference scheme (5.10)

$$\mathcal{A}\mathbf{w}(t) = \mathcal{B}\mathbf{w}'(t) + w(0,t)\mathbf{e_1},$$

where $\mathcal{A}$ and $\mathcal{B}$ are constant sparse matrices independent of the time variable t. Our proposed scheme has its own adaptive regularity, i.e., if at the time instance t, the wave solution $w(\cdot,t) \in C^k([0,1])$, then the corresponding finite difference solution has k-order convergence at t, where $1 \le k \le 6$.

The paper is organized as follows. In Section 2, we provide a general framework for solving the canonical first-order hyperbolic system associated with wave reflections on the boundary. The weak (or generalized) solution is shown to be characterized by two interval mappings that govern the traveling wave and its interaction with the boundary. Based on the results obtained in Section 2, we construct two interval mappings for the Riemann invariant of (1.1) in Section 3. In Section 4, we show that the weak solution of (1.1) can be obtained by the integration of the corresponding Riemann invariant on the boundary and the Gauss-Lobatto integration is proposed for the approximation. Section 5 develops a sixth-order computational scheme for solving (1.1). Several numerical examples are provided in Section 6 to demonstrate the effectiveness of the proposed approaches. The paper ends with concluding remarks in Section 7.

2. First-Order Hyperbolic Systems

In this section, we consider the canonical first-order hyperbolic system

$$\frac{\partial}{\partial t}\begin{bmatrix} u(x,t) \\ v(x,t) \end{bmatrix} = \begin{bmatrix} 1 & 0 \\ 0 & -1 \end{bmatrix} \frac{\partial}{\partial x}\begin{bmatrix} u(x,t) \\ v(x,t) \end{bmatrix}, \qquad 0 < x < 1, \quad t > 0, \tag{2.1}$$

with 'reflected' boundary conditions

$$v(0,t) = \varphi(u(0,t)), \quad u(1,t) = \phi(v(1,t)), \quad t > 0, \tag{2.2}$$

where both ϕ and φ are continuous functions on $\mathbb{R}$. The boundary conditions (2.2) result in wave reflection on the boundary whose dynamics can be characterized by incoming/outgoing characteristic variables. By incoming characteristic we mean a characteristic that enters the domain at the boundary; an outgoing characteristic is one that leaves the domain (see Figure 2).

Definition 2.1. A vector function $(u,v) : [0,T] \to L^\infty([0,1]) \times L^\infty([0,1])$ is a weak solution of (2.1) for $(u(\cdot,0), v(\cdot,0)) = (u_0, v_0) \in L^\infty([0,1]) \times L^\infty([0,1])$ if

(1) for any function $h \in C_0^\infty([0,1] \times [0,T])$ we have

$$\int_0^T \int_0^1 (uh_t - uh_x)dxdt = \int_0^1 hu_0 dx, \quad \int_0^T \int_0^1 (vh_t + vh_x)dxdt = \int_0^1 hv_0 dx$$

and

(2) $v(0,t) = \varphi(u(0,t)), \quad u(1,t) = \phi(v(1,t))$ hold for all $t > 0$.

Theorem 2.1. *The weak solution of the hyperbolic system (2.1) is unique. In other words, (2.1) is well-posed.*

Proof. Suppose that (u_1, v_1) and (u_2, v_2) are two weak solutions of (2.1). Let $\tilde{u} = u_1 - u_2$ and $\tilde{v} = v_1 - v_2$. Then we have $\tilde{u}(x, 0) = \tilde{v}(x, 0) = 0$ and for any function $h \in C_0^\infty([0, 1] \times [0, T])$ we have

$$\int_0^T \int_0^1 (\tilde{u}h_t - \tilde{u}h_x)dxdt = 0, \quad \int_0^T \int_0^1 (\tilde{v}h_t + \tilde{v}h_x)dxdt = 0.$$

Classical result yields that $\tilde{u}$ is a constant along the characteristic $x + t = constant$ and $\tilde{v}$ remains unchanged along the characteristic $x - t = constant$. We first assume $T \leq 1$. For $x + t = c$ with $0 \leq c \leq 1$, we have

$$\tilde{u}(x, t) = \tilde{u}(x + t, 0) = \tilde{u}_0(x + t) = 0,$$

and thus $\tilde{u} \equiv 0$ in $0 \leq x + t \leq 1$. In the region $1 - x \leq t \leq T$, along the characteristic $x + t = c$ with $1 \leq c \leq 2$, we have

$$\begin{aligned} \tilde{u}(x, t) &= \tilde{u}(1, c - 1) = u_1(1, c - 1) - u_2(1, c - 1) = \phi(v_1(1, c - 1)) - \phi(v_2(1, c - 1)) \\ &= \phi(v_1(c, 0)) - \phi(v_2(c, 0)) = \phi(v_0(c)) - \phi(v_0(c)) = 0. \end{aligned}$$

Hence we have $u_1(x, t) = u_2(x, t)$ for $0 \leq t \leq T$.

Similarly, for $x - t = c$ with $0 \leq c \leq 1$, one can see

$$\tilde{v}(x, t) = \tilde{v}(x - t, 0) = \tilde{v}_0(x - t) = 0,$$

which gives $\tilde{v}(x, t) \equiv 0$ in $0 \leq x - t \leq 1$. In the region $x \leq t \leq T$, along $t - x = c$ with $0 \leq c \leq 1$, we have

$$\begin{aligned} \tilde{v}(x, t) &= \tilde{v}(0, c) = v_1(0, c) - v_2(0, c) = \varphi(u_1(0, c)) - \varphi(u_2(0, c)) \\ &= \varphi(u_1(c, 0)) - \varphi(u_2(c, 0)) = \varphi(u_0(c)) - \varphi(u_0(c)) = 0. \end{aligned}$$

Thus, we obtain $v_1(x, t) = v_2(x, t)$ for $0 \leq t \leq T$. When $T \geq 1$, the conclusion now can follow by mathematical induction. □

We next show that under above setting, the hyperbolic system (2.1) will admit a (weak) solution. According to classical theory, the general solution of (2.1) is of the form

$$u(x, t) = f(x + t), \qquad v(x, t) = g(x - t),$$

where f and g are arbitrary functions defined on $\mathbb{R}$. The characteristics $x \pm t$ of (2.1) are the quantities that actually propagate in the flow. The general solution indicates the wave traveling to the left at a unit speed is characterized by u, while the wave moving to the right at the same speed is determined by v. Waves interact at the boundary $x = 0, x = 1$ through functions φ and ϕ. Since the wave speed is one, it is not difficult to see that if a wave reach to the boundary it will hit the boundary again at $t = 2$ with the same moving direction. To see

that, by noting $u(x,t) = f(x+t)$, we immediately have $u(1,0) = f(1) = u(0,1)$ and thus the wave of u starting at $x = 1$ arrives at the left boundary $x = 0$ at $t = 1$. Then it is transformed to the wave of v by $v(0,1) = \varphi(u(0,1))$ at $x = 0$. Since $v(x,t) = g(x-t) = v(1, 1-x+t)$, we have $v(1,2) = v(0,1) = \varphi(u(0,1))$.

Based on the wave reflection, we next construct the solution (u, v) of (2.1). If $0 \le t \le 1-x$, then we have

$$u(x,t) = u(x+t, 0) = u_0(x+t).$$

When $1-x \le t \le 2-x$, by noting that

$$u(x,t) = f(x+t) = u(1, x+t-1)$$

and the boundary condition $u(1,t) = \phi(v(1,t))$, one has

$$u(x,t) = \phi(v(1, x+t-1)) = \phi(v(2-x-t, 0) = \phi(v_0(2-x-t)).$$

Further if $2-x \le t \le 2$, then we have

$$\begin{aligned} u(x,t) = f(x+t) = u(1, x+t-1) = \phi(v(1, x+t-1)) = \phi(v(0, 2-x-t)) \\ = \phi(\varphi(u(0, x+t-2))) = \phi(\varphi(u_0(x+t-2))), \end{aligned}$$

which implies that for $x \in [0,1]$ wave of u goes back to the same location x with the same moving direction at the time $t = 2$. In other words, the wave has a 'period of two' in terms of its dynamics. In summary we have obtained

$$u(x,t) = \begin{cases} u_0(x+t), & t \le 1-x, \\ \phi(v_0(2-x-t)), & 1-x < t \le 2-x, \\ (\phi \circ \varphi)(u_0(x+t-2)), & 2-x < t \le 2. \end{cases} \tag{2.3}$$

Similarly, the wave of v can be discussed in the same way. When $0 \le t \le x$, it is obvious that

$$v(x,t) = g(x-t) = v(x-t, 0) = v_0(x-t).$$

Next when $x \le t \le x+1$, boundary condition $v(0,t) = \varphi(u(0,t))$ yields

$$v(x,t) = g(x-t) = v(0, t-x) = \varphi(u(0, t-x)) = \varphi(u_0(t-x)).$$

When $x+1 \le t \le 2$, both boundary conditions $v(0,t) = \varphi(u(0,t))$ and $u(1,t) = \phi(v(1,t))$ imply

$$\begin{aligned} v(x,t) = g(x-t) = v(0, -x+t) = \varphi(u(0, -x+t)) \\ = \varphi(u(1, -1-x+t)) = \phi(\varphi(v(1, -1-x+t)) = \phi(\varphi(v_0(2+x-t))) \end{aligned}$$

which indicates the the wave starting at x will return to x with the same moving direction at the time $t = 2$. Therefore the solution of v on time interval $0 \le t \le 2$ can be expressed as

$$v(x,t) = \begin{cases} v_0(x-t)), & t \le x, \\ \varphi(u_0(t-x)), & x < t \le 1+x, \\ (\varphi \circ \phi)(v_0(x-t+2)), & 1+x < t \le 2. \end{cases} \tag{2.4}$$

Figure 2 shows how the wave propagates along the characteristics.

More general, we show the existence of the weak solution of (2.1).

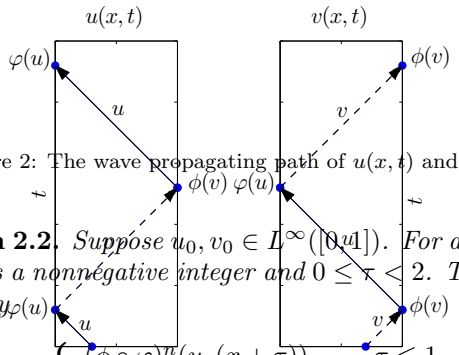

Figure 2: The wave propagating path of $u(x,t)$ and $v(x,t)$ along characteristics.

Theorem 2.2. *Suppose $u_0, v_0 \in L^\infty([0,1])$. For any $t > 0$, we denote $t = 2n+\tau$ where n is a nonnegative integer and $0 \le \tau < 2$. Then the weak solution of (2.1) is given by*

$$u(x,t) = \begin{cases} (\phi\circ\varphi)^n(u_0(x+\tau)), & \tau \le 1-x, \\ (\phi\circ\varphi)^n\left(\phi(v_0(2-x-\tau))\right), & 1-x < \tau \le 2-x, \\ (\phi\circ\varphi)^n\left(\phi\circ\varphi(u_0(x+\tau-2))\right), & 2-x < \tau \le 2, \end{cases} \tag{2.5}$$

and

$$v(x,t) = \begin{cases} (\varphi\circ\phi)^n(v_0(x-\tau)), & \tau \le x, \\ \varphi\circ\phi)^n\left(\varphi(u_0(\tau-x))\right), & x < \tau \le 1+x, \\ (\varphi\circ\phi)^n\left(\varphi\circ\phi(v_0(x-\tau+2))\right), & 1+x < \tau \le 2, \end{cases} \tag{2.6}$$

where $(\varphi\circ\phi)^n$ represents the n-times iterative composition of $\varphi\circ\phi$ with $n = 0,1,2,\ldots$ and $(\varphi\circ\phi)^0 =$identity.

Proof. We have already shown that when $n = 0$ the claim is true. The rest for showing (2.3) and (2.4) follows directly by induction. □

The following corollary states the regularity of the solution of (2.1) whose proof is straightforward.

Corollary 2.1. *Suppose $u_0, v_0 \in C^k([0,1])$ that satisfy the compatible conditions*

$$v_0^{(j)}(0) = \tfrac{d^j}{dx^j}\varphi(u_0(x))\big|_{x=0}, \quad u_0^{(j)}(1) = \tfrac{d^j}{dx}\phi(v_0(x))\big|_{x=1} \tag{2.7}$$

for $j = 0,1,2,\ldots,k$. Then the solution of (2.1) is of class C^k.

3. Iterations of the Riemann Invariant of (1.1)

Based on results presented in previous section, now we are ready to discuss the system (1.1). By Riemann invariants (1.4), the equation (1.1) can be

converted into a *first order hyperbolic* system in the form of

$$\frac{\partial}{\partial t}\begin{bmatrix}u(x,t)\\ v(x,t)\end{bmatrix} = \begin{bmatrix}1 & 0\\ 0 & -1\end{bmatrix}\frac{\partial}{\partial x}\begin{bmatrix}u(x,t)\\ v(x,t)\end{bmatrix}, \qquad 0<x<1, \quad t>0. \tag{3.1}$$

The boundary condition at the left end $x=0$ now becomes

$$u(0,t)+v(0,t) = -\eta[u(0,t)-v(0,t)],$$

or

$$v(0,t) = \frac{\eta+1}{\eta-1}u(0,t), \ t>0, \tag{3.2}$$

and hence we have

$$\varphi(\xi) = \frac{\eta+1}{\eta-1}\xi.$$

While at the right-handed side ($x=1$) the boundary condition satisfies

$$\beta[u(1,t)-v(1,t)]^3 + (1-\alpha)[u(1,t)-v(1,t)] + 2v(1,t) = 0.$$

If $\beta = 0$, then we have

$$u(1,t) = \frac{\alpha+1}{\alpha-1}v(1,t). \tag{3.3}$$

If $\beta \neq 0$, notice that when $0<\alpha<1$ for each given $x\in\mathbb{R}$ the function $y=p(x)$ is well defined through the following implicit cubic equation

$$\beta y^3 + (1-\alpha)y + 2x = 0,$$

by the Cardan's formula

$$y = \sqrt[3]{-\frac{x}{\beta}+\sqrt{\mathcal{D}}} + \sqrt[3]{-\frac{x}{\beta}-\sqrt{\mathcal{D}}},$$

where

$$\mathcal{D} = \frac{(1-\alpha)^3}{27\beta^3} + \frac{x^2}{\beta^2} > 0.$$

Hence we can write

$$u(1,t) = v(1,t) + p(v(1,t)), \ t>0. \tag{3.4}$$

Thus we obtain

$$\phi(\xi) = \xi + p(\xi) \quad \text{if} \quad \beta\neq 0; \quad \text{or} \qquad \phi(\xi) = \frac{\alpha+1}{\alpha-1}\xi \quad \text{if} \quad \beta = 0.$$

The initial conditions are now in the form of

$$u(x,0) = u_0(x) \equiv \frac{w_0'(x)+w_1(x)}{2}, \ v(x,0) = v_0(x) \equiv \frac{w_0'(x)-w_1(x)}{2}. \tag{3.5}$$

According to Theorem 2.2, we have the following:

Theorem 3.1. *The Riemann invariants of (1.1) can be expressed in an iterative form as*

$$u(x,t)=\begin{cases}(\phi\circ\varphi)^n\left(u_0(x+\tau)\right), & \tau\le 1-x,\\ (\phi\circ\varphi)^n\left(\phi(v_0(2-x-\tau))\right), & 1-x<\tau\le 2-x,\\ (\phi\circ\varphi)^{n+1}\left(u_0(x+\tau-2)\right), & 2-x<\tau\le 2,\end{cases}\tag{3.6}$$

and

$$v(x,t)=\begin{cases}(\varphi\circ\phi)^n(v_0(x-\tau)), & \tau\le x,\\ (\varphi\circ\phi)^n(\varphi(u_0(\tau-x))), & x<\tau\le 1+x,\\ (\varphi\circ\phi)^{n+1}(v_0(x-\tau+2)), & 1+x<\tau\le 2,\end{cases}\tag{3.7}$$

where $t=2n+\tau$ with $0\le\tau<2$ and $(\varphi\circ\phi)^n$ represents the n-times iterative composition of $\varphi\circ\phi$.

Using (3.6) and (3.7), u and v of the PDE (3.1) can be represented by the iterations of the maps $\varphi\circ\phi$ and $\phi\circ\varphi$ on $\mathbb{R}$, respectively. The dynamical behavior of u and v can be completely characterized by these two one-dimensional maps.

Since the Riemann invariants of (1.1) is completely determined by the dynamics on $0\le t\le 2$, we here give the explicit solution for $t\in[0,2]$. When $\beta=0$, one has

$$u(x,t)=\begin{cases}u_0(x+t), & t\le 1-x,\\ \frac{\alpha+1}{\alpha-1}v_0(2-x-t), & 1-x<t\le 2-x,\\ \frac{(\alpha+1)(\eta+1)}{(\alpha-1)(\eta-1)}u_0(x+t-2), & 2-x<t\le 2,\end{cases}\tag{3.8}$$

and

$$v(x,t)=\begin{cases}v_0(x-t), & t\le x,\\ \frac{\eta+1}{\eta-1}u_0(t-x), & x<t\le 1+x,\\ \frac{(\alpha+1)(\eta+1)}{(\alpha-1)(\eta-1)}v_0(x-t+2), & 1+x<t\le 2,\end{cases}\tag{3.9}$$

while when $\beta\neq 0$, we have

$$u(x,t)=\begin{cases}u_0(x+t), & t\le 1-x,\\ v_0(2-x-t)+p\left(v_0(2-x-t)\right), & 1-x<\tau\le 2-x,\\ \frac{\eta+1}{\eta-1}u_0(x+t-2)+p\left(\frac{\eta+1}{\eta-1}u_0(x+t-2)\right), & 2-x<t\le 2,\end{cases}\tag{3.10}$$

and

$$v(x,t)=\begin{cases}v_0(x-t), & t\le x,\\ \frac{\eta+1}{\eta-1}u_0(t-x), & x<t\le 1+x,\\ \frac{\eta+1}{\eta-1}\left[v_0(x-\tau+2)+p\left(v_0(x-\tau+2)\right)\right], & 1+x<t\le 2.\end{cases}\tag{3.11}$$

To admit a continuous solution in $C^k([0,1])$, the initial data (u_0, v_0) is required to satisfy compatible conditions (2.7), or directly

$$w_0^{(j)}(0) = -\eta w_1^{(j-1)}(0),\ w_0^{(j)}(1) = \alpha w_1^{(j-1)}(1) - \frac{d^{j-1}}{dx^{j-1}}\left[\beta w_1^3(x)\right]\Big|_{x=1} \quad (3.12)$$

for $j = 1, \ldots, k$.

4. Numerical Integration on the Boundary

From previous section, we have obtained the explicit expression of the Riemann invariants (u, v) of (1.1) and thus (w_x, w_t) can be computed by

$$w_x(x,t) = u(x,t) + v(x,t) \quad \text{and} \quad w_t(x,t) = u(x,t) - v(x,t).$$

Since $w(x,0) = w_0(x)$ and $w_t(x,0) = w_1(x)$ are known, we formally have

$$w(x,t) = \int_0^t [u(x,t) - v(x,t)]dt + w_0(x).$$

The next theorem shows that $w(x,t)$ can be obtained by the integration of the Riemann invariants u at the boundary $x = 0$ and v at $x = 1$, respectively.

Theorem 4.1. *For given $w_0, w_1 \in L^\infty([0,1])$, the weak solution $w \in L^\infty([0,1]\times[0,T])$ of (1.1) can be expressed as*

$$w(x,t) = \int_x^{x+t} u(0,\tau)d\tau - \int_{1-x}^{1-x+t} v(1,\tau)d\tau + w_0(x). \quad (4.1)$$

Moreover, if $w_0 \in C^1([0,1]), w_1 \in C([0,1])$ and the following compatible condition

$$w_0'(0) = -\eta w_1(0), \qquad w_0'(1) = \alpha w_1(1) - \beta w_1^3(1) \quad (4.2)$$

is satisfied, then the solution $w \in C^1([0,1]\times[0,T])$.

In general, if the initial condition $(w_0, w_1) \in C^k([0,1]) \times C^{k-1}([0,1])$ and satisfies the following compatible conditions:

$$w_0^{(j)}(0) = -\eta w_1^{(j-1)}(0),\ w_0^{(j)}(1) = \alpha w_1^{(j-1)}(1) - \frac{d^{j-1}}{dx^{j-1}}\left[\beta w_1^3(x)\right]\Big|_{x=1} \quad (4.3)$$

for $j = 1, 2, \ldots, k$, then the solution $w \in C^k([0,1]\times[0,T])$.

Proof. Let $0 \le x \le 1$ and $t > 0$. Notice that u is constant along its characteristic $x + t = constant$, we have $u(x,t) = u(0, x+t)$. Thus

$$\int_0^t u(x,\tau)d\tau = \int_0^t u(0, x+\tau)d\tau = \int_x^{x+t} u(0,\tau)d\tau.$$

Similarly, v remains constant along its characteristic $t-x = constant$ and hence $v(x,t) = v(1, 1-x+t)$. This yields

$$\int_0^t v(x,\tau)d\tau = \int_0^t v(1,1-x+\tau)d\tau = \int_{1-x}^{1-x+t} v(1,\tau)d\tau.$$

Since $w_0, w_1 \in L^\infty([0,1])$ and φ, ϕ are continuous on $\mathbb{R}$, its Riemann invariants $u, v \in L^\infty([0,1]\times[0,T])$. Therefore the solution

$$\begin{aligned} w(x,t) &= \int_0^t (u(x,t)-v(x,t))dt + w_0(x) \\ &= \int_x^{x+t} u(0,\tau)d\tau - \int_{1-x}^{1-x+t} v(1,\tau)d\tau + w_0(x) \end{aligned}$$

is a function belonging to $L^\infty([0,1]\times[0,T])$. The rest of the proof is straightforward. □

Remark 4.1. We here make some remarks about Theorem 4.1:

(1) In order to obtain the weak solution of (1.1), according to (4.1), one only needs to compute the integrations of $u(0,\tau)$ and $v(1,\tau)$ with respect to the time variable τ.

(2) Suppose that the initial condition (w_0, w_1) does not satisfies the compatible conditions. If (w_0, w_1) is smooth, then both $u(0,\tau)$ and $v(1,\tau)$ are continuous in $(n, n+1)$ but are discontinuous at $n = 0, 1, 2, \ldots$. Let $t = n + s$ with $s \in [0,1)$. Then the integration of u and v can be written, respectively, as

$$\int_x^{x+t} u(0,\tau)d\tau = \left(\int_x^1 + \int_1^2 + \cdots + \int_n^{n+s+x}\right) u(0,\tau)d\tau, \quad \text{for} \quad s+x \le 1$$

or

$$\int_x^{x+t} u(0,\tau)dt = \left(\int_x^1 + \int_1^2 + \cdots + \int_{n+1}^{n+s+x}\right) u(0,\tau)d\tau, \quad \text{for} \quad s+x > 1$$

and

$$\int_{1-x}^{1-x+t} v(1,\tau)d\tau = \left(\int_{1-x}^1 + \int_1^2 + \cdots + \int_n^{1-x+t}\right) v(1,\tau)d\tau, \quad \text{for} \quad s \le x$$

or

$$\int_{1-x}^{1-x+t} v(1,\tau)d\tau = \left(\int_{1-x}^1 + \int_1^2 + \cdots + \int_{n+1}^{1-x+t}\right) v(1,\tau)d\tau, \quad \text{for} \quad s > x.$$

The above decomposition allows us to use methods of high-order integrations on subintervals where either $u(0,\tau)$ or $v(1,\tau)$ is smooth.

Since u and v may have large functional variations, some portions require more attention than others. Thus in order to obtain better accuracy and efficiency for each sub-integral it is necessary to use the adaptive quadrature method [**?** **?** **?**] in which the step size of t can be adjusted to be smaller over portions of the curve u and v where a larger functional variation occurs.

For convenience of description, we denote $\hat{w}(t) = u(0,t)$ or $v(1,t)$ and consider the integration

$$\int_a^b \hat{w}(t)dt.$$

The basic idea behind adaptive quadrature is to integrates

$$\int_a^b \hat{w}(t)dt$$

first by using two different numerical integration methods, thus obtaining the approximations I_1 and I_2. Suppose I_1 is more accurate. Then one uses the relative difference between I_1 and I_2 as an error estimate. If it is less than a given tolerance ϵ, accept I_1 as the answer. Otherwise, divide the interval $[0,T]$ into two subintervals,

$$\int_0^T \hat{w}(t)dt = \int_a^m \hat{w}(t)dt + \int_m^b \hat{w}(t)dt, \quad m = \frac{1}{2}(b-a)$$

and compute the two integrals independently. For each one, compute I_1 and I_2, estimate the error, and continue subdividing if necessary. Dividing any given subinterval stops when its contribution to ϵ is sufficiently small. For instance, one may directly use MATLAB's build in function integral to perform such adaptive quadratures when applicable. To recover the unknowns $w(x_i,T)$ on all uniform spatial grid points, in the first and last sub-intervals of the temporal integrations, we also compositely use the following high-order 7-point Gauss-Kronrod rule [**?**]

$$\begin{aligned}\int_a^b \hat{w}(t)dt \approx \frac{h}{1470}\{&77[\hat{w}(a)+\hat{w}(b)] + 432[\hat{w}(m-\alpha h)+\hat{w}(m+\alpha h)] \\ &+625[\hat{w}(m-\beta h)+\hat{w}(m+\beta h)] + 672\hat{w}(m)\},\end{aligned} \tag{4.4}$$

where

$$h = \frac{1}{2}(b-a), \quad m = \frac{1}{2}(a+b), \quad \alpha = \frac{\sqrt{2}}{\sqrt{3}}, \quad \beta = \frac{1}{\sqrt{5}}.$$

This approach makes possible for us to obtain high order accuracy without compatible assumptions provided that u_0 and v_0 are smooth enough.

Our approach also has advantage for the computation of long-term dynamics of (1.1). To see that, for $0 \le t \le 1$, it is not difficult to see

$$\begin{aligned} w(0,t) &= \int_0^t [u(0,\tau) - v(0,\tau)]d\tau + w_0(0) = \int_0^t [u_0(\tau) - \varphi(u_0(\tau))]\, d\tau + w_0(0) \\ w(1,t) &= \int_0^t [u(1,\tau) - v(1,\tau)]d\tau + w_0(1) = \int_0^t [\phi(v_0(1-t)) - v_0(1-t)]\, d\tau + w_0(1). \end{aligned}$$

Then according to the property of the characteristic quadrilateral of wave equation, for $0 \le x \le 1$, we have

$$w(x,1) = w(0,1-x) + w(1,x) - w_0(1-x),$$

which implies that in order to compute the solution w at $t = 1$, we only need to know the solutions on the boundary $x = 0, 1$ with $0 \le t \le 1$. Similarly, when $t = 2$, we have

$$w(x,2) = w(0,2-x) + w(1,1+x) - w(1-x,1).$$

Note that once the values of $w(0,t)$ and $w(1,t)$ are known for $0 \le t \le 2$, there is no more integration required.

Thus, suppose that we would like to compute the long-term behavior of (1.1). Let $t = n + s$ where $n > 0$ is a positive integer and $0 \le s < 1$. Further, denote the region $\Omega = \{(x,t) : 0 \le x \le 1, n \le t \le n+1\}$. Then we only need to compute $w(0,t)$ and $w(1,t)$ for $0 < t \le n$ in order to obtain $w(x,n)$, and the solution on Ω is given by

$$\begin{aligned} w(x,t) &= \int_n^t [u(x,\tau) - v(x,\tau)]d\tau + w(x,n) \\ &= \int_x^{x+s} u(0,n+\tau)d\tau - \int_{1-x}^{1-x+s} v(1,n+\tau)d\tau + w(x,n). \end{aligned}$$

The significant point here is that to compute the solution on Ω for any $n > 0$, we need not know the solution on $0 < x < 1$, $j-1 < t < j$, $j = 1, \ldots, n$. This greatly reduces the computational complexity if we are only interested in the dynamics near the final time $n \le t \le n + s$.

5. High-order Finite difference approach

In this section, as an alternative, we present an finite difference scheme [**?**] which can give sixth-order accuracy in the spatial variable provided that the compatible conditions (3.12) hold up to $k = 6$.

Let the spatial mesh grid points be

$$x_0 = 0, \quad x_1 = h_x, \ldots, x_j = jh_x, \ldots, x_n = nh_x = 1.$$

For a fixed time t, we denote $w_j = w(x_j, t)$ and

$$w_j^{(k)} = \frac{\partial^k}{\partial x^k} w(x,t)\big|_{x=x_j} \quad \text{for } k = 1, 2, \cdots .$$

According to Taylor's expansions, for any $3 \le j \le n-2$, we have

$$
\begin{aligned}
w_{j+2} &= w_j + 2h_x w_j' + 2h_x^2 w_j'' + \frac{4}{3}h_x^3 w_j''' + \frac{2}{3}h_x^4 w_j^{(4)} + \frac{4}{15}h_x^5 w_j^{(5)} + O(h_x^6)\\
w_{j+1} &= w_j + h_x w_j' + \frac{1}{2}h_x^2 w_j'' + \frac{1}{6}h_x^3 w_j''' + \frac{1}{24}h_x^4 w_j^{(4)} + \frac{1}{120}h_x^5 w_j^{(5)} + O(h_x^6)\\
w_{j-1} &= w_j - h_x w_j' + \frac{1}{2}h_x^2 w_j'' - \frac{1}{6}h_x^3 w_j''' + \frac{1}{24}h_x^4 w_j^{(4)} - \frac{1}{120}h_x^5 w_j^{(5)} + O(h_x^6)\\
w_{j-2} &= w_j - 2h_x w_j' + 2h_x^2 w_j'' - \frac{4}{3}h_x^3 w_j''' + \frac{2}{3}h_x^4 w_j^{(4)} - \frac{4}{15}h_x^5 w_j^{(5)} + O(h_x^6)\\
w_{j-3} &= w_j - 3h_x w_j' + \frac{9}{2}h_x^2 w_j'' - \frac{9}{2}h_x^3 w_j''' + \frac{27}{8}h_x^4 w_j^{(4)} - \frac{81}{40}h_x^5 w_j^{(5)} + O(h_x^6)
\end{aligned}
$$

Thus, it is straightforward to see that

$$1.5w_{j+2} - 15w_{j+1} - 10w_j + 30w_{j-1} - 7.5w_{j-2} + w_{j-3} = -30h_x w_j' + O(h_x^6). \tag{5.1}$$

Similarly, by using Taylor's expansions again, we have

$$
\begin{aligned}
w_{j+2} &= w_{j-1} + 3h_x w_{j-1}' + \frac{9}{2}h_x^2 w_{j-1}'' + \frac{9}{2}h_x^3 w_{j-1}''' + \frac{27}{8}h_x^4 w_{j-1}^{(4)} + \frac{81}{40}h_x^5 w_{j-1}^{(5)} + O(h_x^6)\\
w_{j+1} &= w_{j-1} + 2h_x w_{j-1}' + 2h_x^2 w_{j-1}'' + \frac{4}{3}h_x^3 w_{j-1}''' + \frac{2}{3}h_x^4 w_{j-1}^{(4)} + \frac{4}{15}h_x^5 w_{j-1}^{(5)} + O(h_x^6)\\
w_{j} &= w_{j-1} + h_x w_{j-1}' + \frac{1}{2}h_x^2 w_{j-1}'' + \frac{1}{6}h_x^3 w_{j-1}''' + \frac{1}{24}h_x^4 w_{j-1}^{(4)} + \frac{1}{120}h_x^5 w_{j-1}^{(5)} + O(h_x^6)\\
w_{j-2} &= w_{j-1} - h_x w_{j-1}' + \frac{1}{2}h_x^2 w_{j-1}'' - \frac{1}{6}h_x^3 w_{j-1}''' + \frac{1}{24}h_x^4 w_{j-1}^{(4)} - \frac{1}{120}h_x^5 w_{j-1}^{(5)} + O(h_x^6)\\
w_{j-3} &= w_{j-1} - 2h_x w_{j-1}' + 2h_x^2 w_{j-1}'' - \frac{4}{3}h_x^3 w_{j-1}''' + \frac{2}{3}h_x^4 w_{j-1}^{(4)} - \frac{4}{15}h_x^5 w_{j-1}^{(5)} + O(h_x^6).
\end{aligned}
$$

A linear combination of above equations gives

$$-w_{j+2} + 7.5w_{j+1} - 30w_j + 10w_{j-1} + 15w_{j-2} - 1.5w_{j-3} = 30h_x w_{j-1}' + O(h_x^6). \tag{5.2}$$

The sum of (5.1) and (5.2) yields

$$\tfrac{1}{120}(w_{j-3} - 15w_{j-2} - 80w_{j-1} + 80w_j + 15w_{j+1} - w_{j+2}) = \tfrac{h_x}{2}(w_{j-1}' + w_j') + O(h_x^6) \tag{5.3}$$

for $j = 3, 4, \ldots, n-2$.

Next we establish two more difference equations near the boundary $x = 0$.

Again we apply Taylor's expansions of w at w_0:

$$w_1 = w_0 + h_x w_0' + \frac{1}{2}h_x^2 w_0'' + \frac{1}{6}h_x^3 w_0''' + \frac{1}{24}h_x^4 w_0^{(4)} + \frac{1}{120}h_x^5 w_0^{(5)} + O(h_x^6)$$
$$w_2 = w_0 + 2h_x w_0' + 2h_x^2 w_0'' + \frac{4}{3}h_x^3 w_0''' + \frac{2}{3}h_x^4 w_0^{(4)} + \frac{4}{15}h_x^5 w_0^{(5)} + O(h_x^6)$$
$$w_3 = w_0 + 3h_x w_0' + \frac{9}{2}h_x^2 w_0'' + \frac{9}{2}h_x^3 w_0''' + \frac{27}{8}h_x^4 w_0^{(4)} + \frac{81}{40}h_x^5 w_0^{(5)} + O(h_x^6)$$
$$w_4 = w_0 + 4h_x w_0' + 8h_x^2 w_0'' + \frac{32}{3}h_x^3 w_0''' + \frac{32}{3}h_x^4 w_0^{(4)} + \frac{128}{15}h_x^5 w_0^{(5)} + O(h_x^6)$$
$$w_5 = w_0 + 5h_x w_0' + \frac{25}{2}h_x^2 w_0'' + \frac{125}{6}h_x^3 w_0''' + \frac{625}{24}h_x^4 w_0^{(4)} + \frac{625}{24}h_x^5 w_0^{(5)} + O(h_x^6)$$

which gives

$$-\tfrac{137}{12}w_0 + 25w_1 - 25w_2 + \tfrac{50}{3}w_3 - \tfrac{25}{4}w_4 + w_5 = 5h_x w_0' + O(h_x^6). \tag{5.4}$$

If we expand w at w_1, then we have

$$w_0 = w_1 - h_x w_1' + \frac{1}{2}h_x^2 w_1'' - \frac{1}{6}h_x^3 w_1''' + \frac{1}{24}h_x^4 w_1^{(4)} - \frac{1}{120}h_x^5 w_1^{(5)} + O(h_x^6)$$
$$w_2 = w_1 + h_x w_1' + \frac{1}{2}h_x^2 w_1'' + \frac{1}{6}h_x^3 w_1''' + \frac{1}{24}h_x^4 w_1^{(4)} + \frac{1}{120}h_x^5 w_1^{(5)} + O(h_x^6)$$
$$w_3 = w_1 + 2h_x w_1' + 2h_x^2 w_1'' + \frac{4}{3}h_x^3 w_1''' + \frac{2}{3}h_x^4 w_1^{(4)} + \frac{4}{15}h_x^5 w_1^{(5)} + O(h_x^6)$$
$$w_4 = w_1 + 3h_x w_1' + \frac{9}{2}h_x^2 w_1'' + \frac{9}{2}h_x^3 w_1''' + \frac{27}{8}h_x^4 w_1^{(4)} + \frac{81}{40}h_x^5 w_1^{(5)} + O(h_x^6)$$
$$w_5 = w_1 + 4h_x w_1' + 8h_x^2 w_1'' + \frac{32}{3}h_x^3 w_1''' + \frac{32}{3}h_x^4 w_1^{(4)} + \frac{128}{15}h_x^5 w_1^{(5)} + O(h_x^6)$$

that gives

$$-5w_0 - \tfrac{325}{12}w_1 + 50w_2 - 25w_3 + \tfrac{25}{3}w_4 - \tfrac{5}{4}w_5 = 25h_x w_1' + O(h_x^6). \tag{5.5}$$

By adding (5.4) and (5.5) and then dividing both sides by 30, one can get

$$\begin{array}{l} -\frac{197}{360}w_0 - \frac{25}{360}w_1 + \frac{300}{360}w_2 - \frac{100}{360}w_3 + \frac{25}{360}w_4 - \frac{3}{360}w_5 = \\ \frac{h_x}{6}(w_0' + 5w_1') + O(h_x^6) \end{array} \tag{5.6}$$

By using the same technique, one can have

$$\tfrac{1}{180}(-6w_0 - 125w_1 + 80w_2 + 60w_3 - 10w_4 + w_5) = \tfrac{h_x}{3}(w_1' + 2w_2') + O(h_x^6) \tag{5.7}$$

Similarly, we establish another two equations near the boundary $x = 1$ as

$$\begin{array}{l} \frac{1}{180}(-w_{n-5} + 10w_{n-4} - 60w_{n-3} - 80w_{n-2} + 125w_{n-1} + 6w_n) = \\ \frac{h_x}{3}(2w_{n-2}' + w_{n-1}') + O(h_x^6) \end{array} \tag{5.8}$$

and

$$\begin{array}{l} \frac{1}{360}(3w_{n-5} - 25w_{n-4} + 100w_{n-3} - 300w_{n-2} + 25w_{n-1} + 197w_n) = \\ \frac{h_x}{6}(5w_{n-1}' + w_n') + O(h_x^6). \end{array} \tag{5.9}$$

In summary, we have obtained the following approximated difference equations with sixth-order accuracy:

$$\frac{1}{120}(w_{j-3} - 15w_{j-2} - 80w_{j-1} + 80w_j + 15w_{j+1} - w_{j+2}) = \frac{h_x}{2}(w'_{j-1} + w'_j)$$

for $j = 3, 4, \ldots, n-2$, and four equations near the boundaries

$$\frac{1}{360}(-197w_0 - 25w_1 + 300w_2 - 100w_3 + 25w_4 - 3w_5) = \frac{h_x}{6}(w'_0 + 5w'_1)$$

$$\frac{1}{180}(-6w_0 - 125w_1 + 80w_2 + 60w_3 - 10w_4 + w_5) = \frac{h_x}{3}(w'_1 + 2w'_2)$$

$$\frac{1}{180}(-w_{n-5} + 10w_{n-4} - 60w_{n-3} - 80w_{n-2} + 125w_{n-1} + 6w_n) = \frac{h_x}{3}(2w'_{n-2} + w'_{n-1})$$

$$\frac{1}{360}(3w_{n-5} - 25w_{n-4} + 100w_{n-3} - 300w_{n-2} + 25w_{n-1} + 197w_n) = \frac{h_x}{6}(5w'_{n-1} + w'_n).$$

Next we compute $w_0 = w(0,t)$ by integration over the boundary $x = 0$. By the boundary condition at $x = 0$, we have

$$w_0 = \int_0^t [u(0,\tau) - v(0,\tau)]d\tau + w_0(0) = \frac{2}{\eta - 1}\int_0^t u(0,\tau)d\tau + w_0(0),$$

which can be computed efficiently via, for example, adaptive quadrature method. We remark that the error in above quadrature is the only temporal error in this scheme. Notice that for $j = 0, 1, 2, \ldots, n$ we already know

$$w'_j = \frac{\partial}{\partial x}w(x,t)\big|_{x=x_j} = u(x_j,t) + v(x_j,t),$$

where $u(x_j,t)$ and $v(x_j,t)$ are computed by (3.6) and (3.7), respectively.

For clarity, we denote

$$\mathbf{w}(t) \quad = \quad [w_0, w_1, w_2, \ldots, w_n]^T, \quad \mathbf{w}'(t) = [w'_0, w'_1, w'_2, \ldots, w'_n]^T,$$

and then gather all above approximations in to the following linear system

$$\mathcal{A}\mathbf{w}(t) = \mathcal{B}\mathbf{w}'(t) + w_0\mathbf{e_1}, \tag{5.10}$$

where

$$\mathcal{A} = \begin{bmatrix} 1 & 0 & 0 & 0 & 0 & 0 & \cdots & 0 \\ -197/360 & -25/360 & 300/360 & -100/360 & 25/360 & -3/360 & \ddots & 0 \\ -6/180 & -125/180 & 80/180 & 60/180 & -10/180 & 1/180 & \ddots & 0 \\ 1/120 & -15/120 & -80/120 & 80/120 & 15/120 & -1/120 & \ddots & 0 \\ 0 & \ddots & \ddots & \ddots & \ddots & \ddots & \ddots & 0 \\ 0 & \ddots & 1/120 & -15/120 & -80/120 & 80/120 & 15/120 & -1/120 \\ 0 & \ddots & -1/180 & 10/180 & -60/180 & -80/180 & 125/180 & 6/180 \\ 0 & \ddots & 3/360 & -25/360 & 100/360 & -300/360 & 25/360 & 197/360 \end{bmatrix},$$

$$\mathcal{B} = \begin{bmatrix} 0 & 0 & 0 & 0 & 0 & 0 & 0 & 0 & 0 \\ 1/6 & 5/6 & 0 & \ddots & \ddots & \ddots & \ddots & \ddots & \ddots \\ 0 & 1/3 & 2/3 & 0 & \ddots & \ddots & \ddots & \ddots & \ddots \\ 0 & 1 & 1 & 0 & \ddots & \ddots & \ddots & \ddots & \ddots \\ 0 & \ddots & \ddots & \ddots & \ddots & \ddots & \ddots & \ddots & 0 \\ 0 & \ddots & \ddots & \ddots & \ddots & 0 & 1 & 1 & 0 \\ 0 & \ddots & \ddots & \ddots & \ddots & 0 & 2/3 & 1/3 & 0 \\ 0 & \ddots & \ddots & \ddots & \ddots & \ddots & 0 & 5/6 & 1/6 \end{bmatrix},$$

and $\mathbf{e_1}$ is first column of identity matrix with dimension $(n+1)$. The nice feature of this approach is that we can obtain the approximated solution on any time instance without requiring any explicit information of prior time solution except at the left boundary $x = 0$. This sixth-order finite difference scheme (FD-6) turns out to be very efficient since it only needs a boundary integration to approximate $w(0,t)$ and then a linear system solving. This approach minimizes the error accumulation in a significant way. Moreover, the approach remains valid even if the solution $w \in C^k([0,1] \times [0,T])$ for $1 \leq k < 6$, since in that case we still have Taylor expansion up to $k+1$ term, and of course the convergence will be kth-order. In general, its high-order accuracy relies on the regularity of compatibility conditions. The higher regularity of compatibility conditions holds, the higher order accuracy it will be attained.

6. Numerical Examples

In this section we present numerical tests with three different methods developed in our paper. All experiments are implemented using MATLAB 2013a on a Laptop PC with Intel(R) Core(TM) i3-3120M CPU @ 2.50GHz. In discretization we choose identical spatial and temporal step size $h = \Delta x = \Delta t$. Denote by $w_h(x_i, t_j)$ the approximated solution to $w(x,t)$ at grid point (x_i, t_j) with $x_i = ih$ and $t_j = jh$. When the exact solutions are unknown, we use the approximation $w_Q(x,t)$ obtained by our proposed boundary integration method (BIM) with the computed finest mesh (e.g. $h = 1/5120$) as the benchmark reference. Otherwise, we will use the analytic formula as the reference. In particular, we measure the maximum absolute error E_h of current approximation $w_h(x,T)$ by subtracting it from the reference values over their shared spatial grid points at final time T. As in [**?**], the experimental order of convergence can be estimated by

$$\mathrm{R} = \log_2 \left(\frac{E_{2h}}{E_h} \right),$$

which equals 2 for the second order scheme (FD-2) and 6 for the sixth order scheme (FD-6). In particular, the FD-6 sparse linear system can be solved

efficiently by existing linear algebra method, and the integration can be obtained by adaptive quadrature technique.

6.1. Example 1.

We first consider a simple case: $\beta = 0$ and the initial conditions are

$$w_0(x) = -\cos(x) \quad \text{and} \quad w_1(x) = \sin(x),$$

which gives

$$u_0(x) = \sin(x) \quad \text{and} \quad v_0(x) = 0.$$

It follows from $\beta = 0$ that $\phi \circ \varphi = \varphi \circ \phi$ is just a scalar multiplication. We denote the corresponding scalar by $\gamma := \frac{(\alpha+1)(\eta+1)}{(\alpha-1)(\eta-1)}$. Notice that with $\alpha = 1/2, \eta = -2$ we would get $\gamma = -1$. By expressions (3.6) and (3.7), for any $t = 2n + r$ with $0 \le r \le 2$, we have (notice we used $v_0(x) = 0$)

$$u(x,t) = \begin{cases} \gamma^n \sin(x+r), & r \le 1-x, \\ 0, & 1-x < r \le 2-x, \\ \gamma^{n+1} \sin(x+r-2), & 2-x < r \le 2, \end{cases} \tag{6.1}$$

and

$$v(x,t) = \begin{cases} 0, & r \le x, \\ \frac{\eta+1}{\eta-1}\gamma^n \sin(r-x), & x < r \le 1+x, \\ 0, & 1+x < r \le 2. \end{cases} \tag{6.2}$$

Thus we could obtain

$$\int_x^{x+t} u(0,\tau)d\tau =$$

$$\begin{cases} \cos(x) - \cos(x+t), & \text{if } x+t \le 1 \\ \cos(x) - \cos(1), & \text{if } 1 < x+t \le 2 \\ \cos(x) - \cos(1) + \gamma[1 - \cos(x+t-2)], & \text{if } 2 < x+t \le 3 \\ \cos(x) - \cos(1) + \gamma[1 - \cos(1)], & \text{if } 3 < x+t \le 4 \\ \cos(x) - \cos(1) + \gamma[1 - \cos(1)] + \gamma^2[1 - \cos(x+t-4)], & \text{if } 4 < x+t \le 5 \\ \cos(x) - \cos(1) + \gamma[1 - \cos(1)] + \gamma^2[1 - \cos(1)], & \text{if } 5 < x+t \le 6 \end{cases}$$

and

$$\int_{1-x}^{1-x+t} v(1,\tau)d\tau =$$

$$\begin{cases} 0, & \text{if } t-x \le 0 \\ \frac{\eta+1}{\eta-1}[1 - \cos(t-x)], & \text{if } 0 < t-x \le 1 \\ \frac{\eta+1}{\eta-1}[1 - \cos(1)], & \text{if } 1 < t-x \le 2 \\ \frac{\eta+1}{\eta-1}\{[1 - \cos(1)] + \gamma[1 - \cos(t-x-2)]\}, & \text{if } 2 < t-x \le 3 \\ \frac{\eta+1}{\eta-1}\{[1 - \cos(1)] + \gamma[1 - \cos(1)]\}, & \text{if } 3 < t-x \le 4 \\ \frac{\eta+1}{\eta-1}\{[1 - \cos(1)] + \gamma[1 - \cos(1)] + \gamma^2[1 - \cos(t-x-4)]\}, & \text{if } 4 < t-x \le 5 \\ \frac{\eta+1}{\eta-1}\{[1 - \cos(1)] + \gamma[1 - \cos(1)] + \gamma^2[1 - \cos(1)]\}, & \text{if } 5 < t-x \le 6 \end{cases}$$

Here we only give the expression up to $t = 5$ for simplicity. Above calculations can be repeated for any t. Finally, the exact solution is given by Theorem 4.1.

In Tables 1 and 2 we report the error results and computation time of three different methods with $T = 6$ and $T = 7$. It is clear that violating compatibility condition reduces FD-2 method to be only first order accurate. While the convergence order of our FD-6 method depends on whether $w(x, T)$ crosses non-smooth points in space. The FD-6 method will be also first order accurate in presence of non-smooth points (see Table 2), but it recovers its sixth order accuracy if there are no non-smooth points (see Table 1). Here we used above analytic solution as reference, the 'Error' columns show that our BIM achieves a machine-level accuracy, which is attribute to the employed highly accurate Gauss-Lobatto rule. Thus, it is reasonable to use our proposed quadrature method as reference in the following examples without known analytic solutions. The 'CPU' columns illustrate that both our FD-6 method and BIM are much faster than the FD-2 method as mesh refines.

Table 1: Errors for solving Example 1 with $T = 6$ ($\beta = 0, \alpha = 1/2, \eta = -2$).

	FD-2			Our FD-6			Our BIM		
$1/h$	Error	R	CPU	Error	R	CPU	Error	R	CPU
20	1.6e-02	1.2	0.003	1.3e-11	6.5	0.005	3.3e-16		0.007
40	7.6e-03	1.1	0.006	1.7e-13	6.3	0.005	4.4e-16		0.008
80	3.7e-03	1.1	0.013	2.7e-15	6.0	0.005	4.4e-16		0.007
160	1.8e-03	1.0	0.029	4.1e-15		0.005	4.4e-16		0.009
320	8.9e-04	1.0	0.059	8.3e-15		0.005	1.0e-15		0.008
640	4.4e-04	1.0	0.146	1.7e-14		0.006	1.0e-15		0.010
1280	2.2e-04	1.0	0.367	3.6e-14		0.007	8.9e-16		0.011
2560	1.1e-04	1.0	1.117	7.6e-14		0.011	1.6e-15		0.018

Table 2: Errors for solving Example 1 with $T = 7$ ($\beta = 0, \alpha = 1/2, \eta = -2$).

	FD-2			Our FD-6			Our BIM		
$1/h$	Error	R	CPU	Error	R	CPU	Error	R	CPU
20	6.1e-03	0.8	0.004	1.4e-02	1.0	0.005	2.2e-16		0.009
40	3.3e-03	0.9	0.007	6.9e-03	1.0	0.005	2.2e-16		0.008
80	1.7e-03	1.0	0.015	3.4e-03	1.0	0.007	2.2e-16		0.008
160	8.6e-04	1.0	0.032	1.7e-03	1.0	0.005	4.4e-16		0.009
320	4.3e-04	1.0	0.071	8.6e-04	1.0	0.006	6.7e-16		0.009
640	2.2e-04	1.0	0.184	4.3e-04	1.0	0.006	4.4e-16		0.010
1280	1.1e-04	1.0	0.485	2.1e-04	1.0	0.008	4.4e-16		0.017
2560	5.5e-05	1.0	1.261	1.1e-04	1.0	0.010	6.7e-16		0.018

6.2. Example 2.

In this example, the initial conditions are the same as in Example 1 and the test parameters are $\beta = 1, \alpha = 1/2, \eta = 1/2$. Notice that the presence

of nonlinear term will complicate the dynamics of the solution. The results in Table 3 demonstrate the high-order accuracy of our BIM without assuming any compatibility conditions. Again the FD-2 and FD-6 methods attain only first-order accuracy, but our FD-6 method still achieves better accuracy with much less CPU time. Moreover, our BIM has significant advantage over both FD-2 and FD-6 methods in the sense that it can provide much higher accuracy, which would be crucial in the simulations of long-term dynamics.

Table 3: Errors for solving Example 2 with $T = 6.5$ ($\beta = 1, \alpha = 1/2, \eta = 1/2$).

	FD-2			Our FD-6			Our BIM		
$1/h$	Error	R	CPU	Error	R	CPU	Error	R	CPU
20	3.4e-01	1.1	0.004	3.7e-02	2.2	0.021	2.6e-03	1.9	0.050
40	1.2e-01	1.5	0.007	2.4e-02	0.6	0.021	2.3e-04	3.5	0.051
80	4.4e-02	1.4	0.014	6.7e-03	1.9	0.021	4.3e-05	2.4	0.050
160	2.2e-02	1.0	0.030	2.3e-03	1.5	0.022	3.7e-06	3.5	0.053
320	1.2e-02	0.9	0.076	1.1e-03	1.1	0.029	9.6e-07	2.0	0.057
640	6.0e-03	1.0	0.190	7.6e-04	0.5	0.025	1.6e-08	5.9	0.070
1280	3.1e-03	1.0	0.455	4.8e-04	0.7	0.043	6.8e-10	4.6	0.074
2560	1.6e-03	1.0	1.242	2.7e-04	0.8	0.032	6.2e-12	6.8	0.123
5120	8.0e-04	1.0	3.943	1.4e-04	0.9	0.039			0.240

To demonstrate the FD-2 method may provide much worse convergence, we only adjust the parameter $\alpha = 0.99$ and re-run the simulations. In Table 4 we report the error results with a little longer time $T = 13$. The corresponding approximated solutions $w(x, T = 13)$ are plotted in Figure 3. The approximations from FD-2 method will not be acceptable, even for the finest mesh.

Table 4: Errors for solving Example 2 with $T = 13$ ($\beta = 1, \alpha = .99, \eta = 1/2$).

	FD-2			Our FD-6			Our BIM		
$1/h$	Error	R	CPU	Error	R	CPU	Error	R	CPU
20	3.3	-0.6	0.007	2.8e-01	-0.0	0.201	3.1e-02	1.6	0.744
40	5.6	-0.8	0.021	7.0e-02	2.0	0.207	9.8e-03	1.7	0.697
80	2.1	1.4	0.029	5.7e-02	0.3	0.201	2.0e-02	-1.1	0.684
160	1.1	1.0	0.063	2.8e-02	1.0	0.204	1.1e-02	1.0	0.684
320	1.9	-0.8	0.139	1.8e-02	0.7	0.210	4.4e-03	1.3	0.643
640	4.0	-1.1	0.335	5.4e-03	1.7	0.206	9.0e-04	2.3	0.657
1280	3.9	0.1	0.848	4.1e-03	0.4	0.216	4.0e-04	1.2	0.658
2560	0.38	3.3	2.417	1.5e-03	1.4	0.218	2.7e-04	0.6	0.637
5120	0.54	-0.5	7.900	7.0e-04	1.1	0.220			0.831

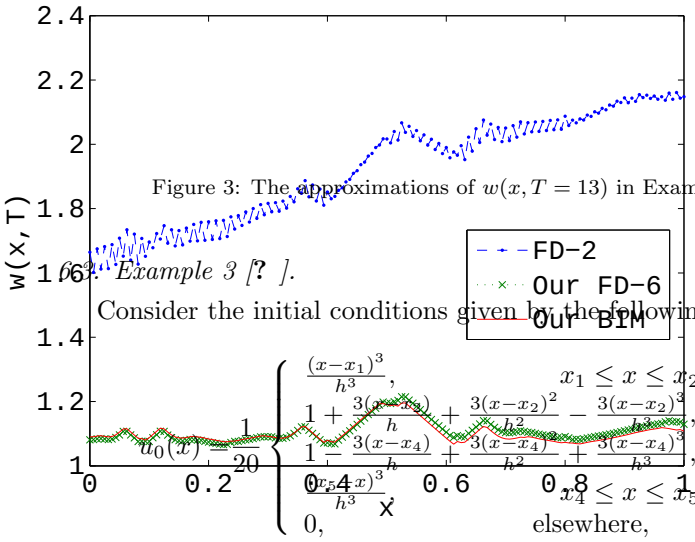

Figure 3: The approximations of $w(x, T = 13)$ in Example 2 ($h = 1/160$).

6.3. *Example 3 [?].*

Consider the initial conditions given by the following C^2-*spline functions*:

$$u_0(x) = \frac{1}{20}\begin{cases} \frac{(x-x_1)^3}{h^3}, & x_1 \le x \le x_2, \\ 1 + \frac{3(x-x_2)}{h} + \frac{3(x-x_2)^2}{h^2} - \frac{3(x-x_2)^3}{h^3}, & x_2 \le x \le x_3, \\ 1 - \frac{3(x-x_4)}{h} + \frac{3(x-x_4)^2}{h^2} + \frac{3(x-x_4)^3}{h^3}, & x_3 \le x \le x_4, \\ \frac{(x_5-x)^3}{h^3}, & x_4 \le x \le x_5, \\ 0, & \text{elsewhere}, \end{cases}$$

and

$$v_0(x) = \frac{1}{20}\begin{cases} \frac{(x-y_1)^3}{h^3}, & y_1 \le x \le y_2, \\ 1 + \frac{3(x-y_2)}{h} + \frac{3(x-y_2)^2}{h^2} - \frac{3(x-y_2)^3}{h^3}, & y_2 \le x \le y_3, \\ 1 - \frac{3(x-y_4)}{h} + \frac{3(x-y_4)^2}{h^2} + \frac{3(x-y_4)^3}{h^3}, & y_3 \le x \le y_4, \\ \frac{(y_5-x)^3}{h^3}, & y_4 \le x \le y_5, \\ 0, & \text{elsewhere}, \end{cases}$$

where $h = \frac{1}{5}$, $x_i = \frac{i}{5}$, $y_i = \frac{i-1}{5}$, $i = 1, 2, 3, 4, 5$. Notice that above initial conditions satisfy the compatibility condition up to first order, which implies FD-2 method would give a second-order accuracy. The error results for Example 3 with $T = 6$ and $T = 14$ are given in Table 5 and 6, respectively. In Table 5, as expected, we observe a clear second-order accuracy for the FD-2 method. However, with $T = 14$, it fails to give a clear second-order accuracy within computed mesh size. Our proposed BIM and FD-6 method keep its high-order accuracy,

which greatly outperform FD-2 method. In Figure 4 we plotted the computed approximations $w(x,T)$ with different methods to emphasize the possible large approximation error of the FD-2 method. We remark that for this particular example both $w_x(x,t)$ and $w_t(x,t)$ undergo chaotic fluctuations as T increases, which in return will bring challenges to traditional finite difference methods.

Table 5: Errors for solving Example 3 with $T = 6$ ($\beta = 1, \alpha = 1/2, \eta = 0.55$).

	FD-2			Our FD-6			Our BIM		
$1/h$	Error	R	CPU	Error	R	CPU	Error	R	CPU
20	1.6e-01	1.0	0.004	6.3e-03	3.9	0.016	3.9e-07	7.0	0.030
40	5.7e-02	1.5	0.007	1.3e-03	2.3	0.016	9.5e-10	8.7	0.030
80	1.5e-02	2.0	0.013	4.7e-05	4.7	0.015	4.6e-12	7.7	0.031
160	3.7e-03	2.0	0.029	3.1e-07	7.2	0.016	1.6e-15	11.5	0.032
320	9.4e-04	2.0	0.065	1.8e-08	4.1	0.018	2.0e-15		0.034
640	2.3e-04	2.0	0.160	6.2e-09	1.5	0.018	2.3e-15		0.040
1280	5.9e-05	2.0	0.397	5.5e-09	0.2	0.022	1.8e-15		0.054
2560	1.5e-05	2.0	1.146	5.5e-09	0.0	0.025	1.3e-15		0.068
5120	3.7e-06	2.0	3.659	5.5e-09	0.0	0.035			0.258

Table 6: Errors for solving Example 3 with $T = 14$ ($\beta = 1, \alpha = 1/2, \eta = 0.55$).

	FD-2			Our FD-6			Our BIM		
$1/h$	Error	R	CPU	Error	R	CPU	Error	R	CPU
20	4.6e-01	-1.1	0.008	1.6e-01	-0.1	0.098	2.1e-02	1.9	0.177
40	2.8e-01	0.7	0.016	5.0e-02	1.7	0.100	4.6e-03	2.2	0.183
80	2.5e-01	0.2	0.031	1.9e-02	1.4	0.098	1.5e-04	5.0	0.182
160	1.4e-01	0.8	0.069	2.0e-02	-0.0	0.098	8.5e-06	4.1	0.190
320	7.7e-02	0.9	0.154	1.6e-03	3.7	0.102	1.7e-07	5.7	0.196
640	1.2e-01	-0.7	0.361	2.0e-04	3.0	0.100	5.8e-10	8.2	0.199
1280	1.4e-01	-0.2	0.886	1.1e-05	4.2	0.104	3.3e-12	7.5	0.203
2560	9.0e-02	0.6	2.650	1.7e-07	6.0	0.111	1.1e-13	4.8	0.232
5120	2.8e-02	1.7	9.170	1.7e-09	6.6	0.121			0.452

*6.4. Example 4 [**?**].*

In this example we choose the initial conditions

$$w_0(x) = 0.2\sin\left(\frac{\pi}{2}x\right), \quad w_1(x) = 0.2\sin(\pi x),$$

which give

$$u_0(x) = 0.1\left[\frac{\pi}{2}\cos\left(\frac{\pi}{2}x\right) + \sin(\pi x)\right], \quad v_0(x) = 0.1\left[\frac{\pi}{2}\cos\left(\frac{\pi}{2}x\right) - \sin(\pi x)\right].$$

The parameters are set as $\beta = 1, \alpha = 1/2, \eta = 1.52$ to test the chaotic dynamics [**?**]. In this case, the compatible condition (4.2) hold up to only first order.

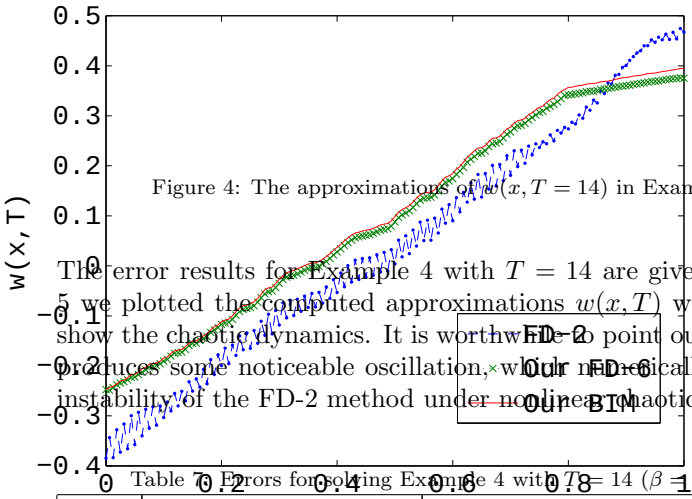

Figure 4: The approximations of $w(x, T = 14)$ in Example 3 ($h = 1/160$).

The error results for Example 4 with $T = 14$ are given in Table 7. In Figure 5 we plotted the computed approximations $w(x, T)$ with different methods to show the chaotic dynamics. It is worthwhile to point out that the FD-2 method produces some noticeable oscillation, which numerically indicates the possible instability of the FD-2 method under nonlinear chaotic dynamics.

Table 7: Errors for solving Example 4 with $T = 14$ ($\beta = 1, \alpha = 1/2, \eta = 1.52$).

	FD-2			Our FD-6			Our BIM		
$1/h$	Error	R	CPU	Error	R	CPU	Error	R	CPU
20	1.8	-0.6	0.007	3.3e-01	0.4	0.280	4.6e-02	0.2	0.519
40	1.0	0.8	0.015	1.6e-01	1.0	0.253	2.8e-02	0.7	0.528
80	4.5e-01	1.2	0.031	1.9e-01	-0.3	0.243	3.0e-02	-0.1	0.457
160	2.0e-01	1.2	0.066	8.8e-02	1.1	0.244	5.4e-03	2.4	0.459
320	1.0e-01	1.0	0.147	5.8e-02	0.6	0.244	6.9e-03	-0.4	0.463
640	4.3e-02	1.2	0.349	2.1e-02	1.5	0.251	1.4e-03	2.4	0.465
1280	2.4e-02	0.8	0.887	8.2e-03	1.3	0.285	7.5e-04	0.9	0.542
2560	2.0e-02	0.3	2.644	3.0e-03	1.5	0.259	3.9e-04	1.0	0.618
5120	6.4e-03	1.7	8.685	1.2e-03	1.3	0.350			0.693

7. Concluding remarks

In this paper, we provide numerical methods for solving the wave equation with van der Pol type boundary condition. Due to the complexity of the system

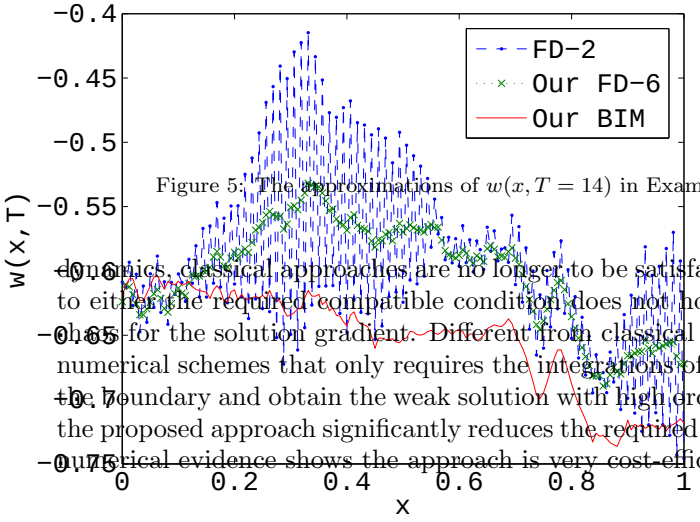

Figure 5: The approximations of $w(x, T = 14)$ in Example 4($h = 1/160$).

dynamics, classical approaches are no longer to be satisfactory in most cases due to either the required compatible condition does not hold or the occurrence of chaos for the solution gradient. Different from classical approaches, we develop numerical schemes that only requires the integrations of Riemann invariants on the boundary and obtain the weak solution with high order accuracy. Moreover, the proposed approach significantly reduces the required computational cost and numerical evidence shows the approach is very cost-efficient.